Supporting Information

Synthesis of bifunctional fluorescent nanohybrids of carbon dots–copper nanoclusters via a facile method for Fe^{3+} and Tb^{3+} ratiometric detection

Shumin Lin,[a]* Jiangxue Dong,[b]* Bangwen Zhang,[a] Zeming Yuan,[a] Chunxiao Lu,[a] Pei Han,[a] Jia Xu,[a] Lina Jia,[a] and Li Wang[a]

[a] *Analysis and Testing Center, Inner Mongolia University of Science and Technology, Baotou, 014010, PR China*

[b] *College of Chemistry and Environmental Science, Hebei University, Key Laboratory of Analytical Science and Technology of Hebei Province, Baoding, 071002, PR China*

[*] Corresponding author

[*] Shumin Lin and Jiangxue Dong

E–mail address: lsmnmg@126.com; dongjx@hbu.edu.cn

[*] Aerding Road, Kundulun District, Baotou, 014010, PR China.

Contents

Experimental section

Materials. Copper nitrate ($Cu(NO_3)_2•3H_2O$), D-penicillamine (DPA) and L-ascorbic acid (AA) were purchased from Macklin Chemical Reagents Co., Ltd., Shanghai, China. Aqueous solutions of Na^+, Mg^{2+}, Ba^{2+}, K^+, Ca^{2+}, Co^{2+}, Al^{3+}, Mn^{2+}, Pb^{2+}, Li^+, Zn^{2+}, Fe^{2+}, Cr^{3+}, Cu^{2+}, Hg^{2+}, and Fe^{3+} were prepared from NaCl, $MgCl_2•6H_2O$, $BaCl_2•2H_2O$, KCl, $CaCl_2•2H_2O$, $Co(NO_3)_2•6H_2O$, $Al(NO_3)_3•9H_2O$, $MnCl_2•4H_2O$, $Pb(NO_3)_2$, $LiNO_3$, $Zn(NO_3)_2•6H_2O$, $Fe(NO_3)_2•6H_2O$, $CrN_3O_9•9H_2O$, $Cu(NO_3)_2•3H_2O$, $Hg(NO_3)_2•H_2O$, and $Fe(NO_3)_3•9H_2O$, respectively. Aqueous solutions of (La^{3+}, Ce^{2+}, Pr^{3+}, Nd^{3+}, Sm^{3+}, Eu^{3+}, Gd^{3+}, Er^{3+}, Tb^{3+}, Ho^{3+}, Tm^{3+}, Yb^{3+}, Lu^{3+} and Y^{3+} were prepared from $LaCl_3$, $Ce(SO_4)_2$, $PrCl_3$, $NdCl_3$, $SmCl_3$, $EuCl_3$, $GdCl_3$, $Er(NO_3)_3•5H_2O$, $Tb(NO_3)_3•5H_2O$, $Ho(NO_3)_3•5H_2O$, $Tm(NO_3)_3•6H_2O$, $YbCl_3$, $LuCl_3$ and YCl_3, respectively. In addition, Britton-Robinson (BR) buffer (10 mM), KH_2PO_4-$Na_2B_4O_7$ buffer (0.1 M), KH_2PO_4-NaOH buffer (0.1 M), and KH_2PO_4-Na_2HPO_4 buffer (0.1 M) were prepared. Ultrapure water (18.2 MΩ cm) was used throughout all the experiments. All solvents were of analytical reagent grade and were freshly prepared.

Instruments. All fluorescence measurements were performed using a Hitachi F-2700 spectrofluorophotometer (Tokyo, Japan) with excitation and emission slits of 10 nm in a 1 cm × 1 cm quartz cell. UV-vis absorption spectra were recorded with a U-3900 spectrophotometer (Hitachi, Japan). High-resolution transmission electron microscopy (HR-TEM) and TEM images were recorded with a JEM-2100F equipment (Japan). An 85-2 constant temperature magnetic mixer (Zongda Instrument

Plant, Jiangsu, China) was used to mix solution completely. X-ray photoelectron spectroscopy (XPS) spectra were performed with an ESCALAB 250Xi X-ray photoelectron spectroscopy (Thermo Electron, USA). The Fourier transform infrared (FTIR) analysis was achieved on a TENSOR Ⅱ (Bruker, Germany) 113v spectrometer. Fluorescence lifetime decays were measured using an Edinburgh FL 1000 fluorescence spectrometer (Edinburgh, U.K.). X-ray powder diffraction patterns were obtained on Smartlab X-ray powder diffraction instrument (Rigaku Corporation, Japan). Zeta potential measurements were conducted on 90Plus PALS instrument (Brookhaven, USA).

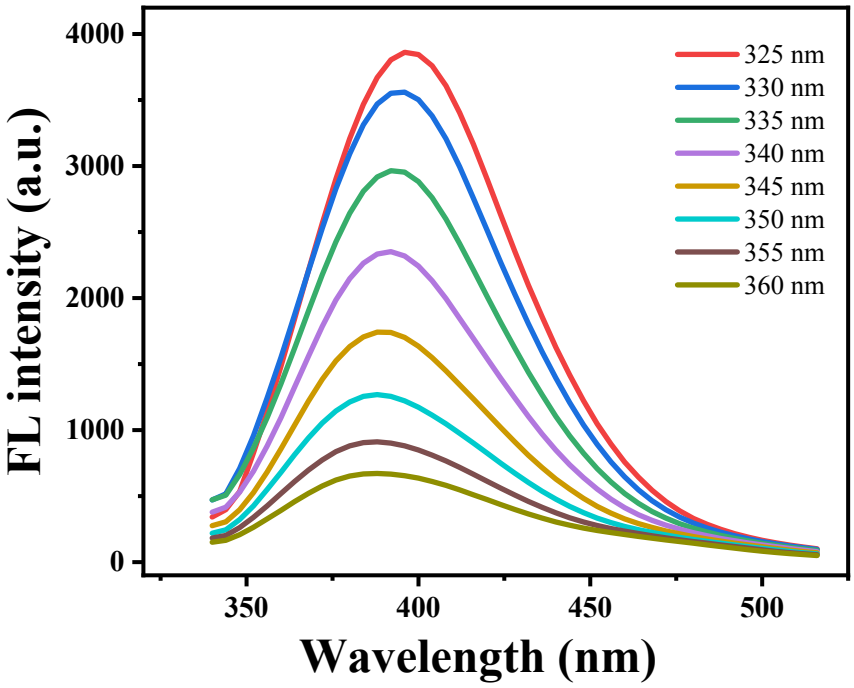

Fig. S1. Fluorescence emission spectra of CDs (3.6 mg mL^{-1})) under different excitations.

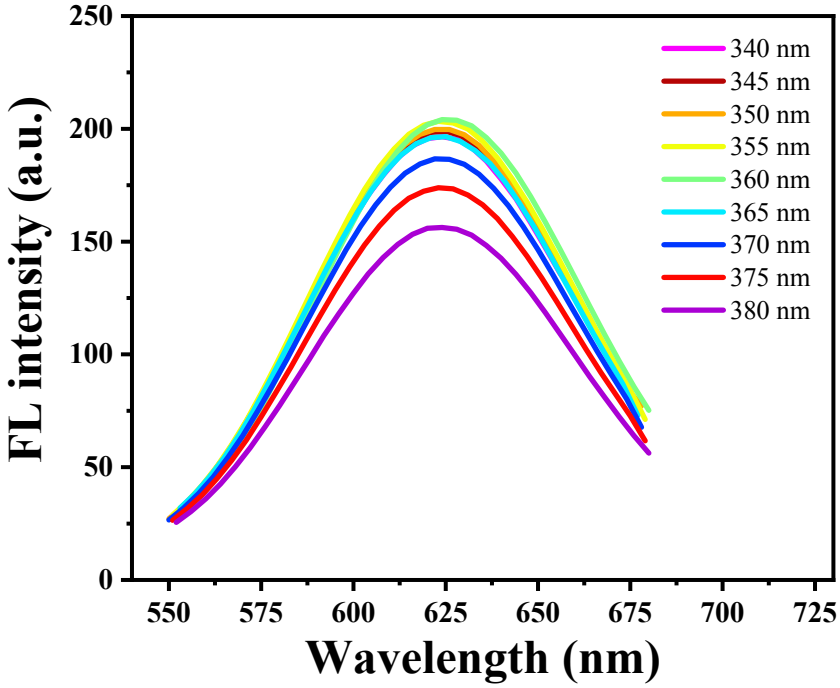

Fig. S2. Fluorescence emission spectra of Cu NCs (10.0 mg mL^{-1})) under different excitations.

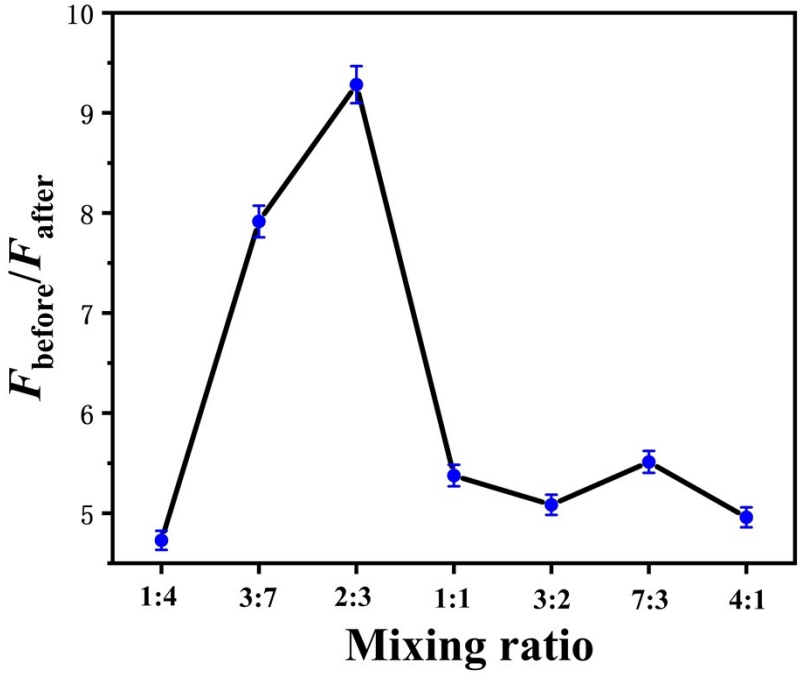

Fig. S3. The quenching efficiency to Fe^{3+} with different mixing ratio (1:4; 3:7; 2:3; 1:1; 3:2; 7:3; 4:1) of CDs and Cu NCs. In which F_{before} represent the ratio fluorescence intensities of CDs–Cu NCs (F_{624}/F_{424}) before addition of Fe^{3+}; F_{after} represent the ratio fluorescence intensities of CDs–Cu NCs (F_{624}/F_{424}) after addition of Fe^{3+} (40 μM).

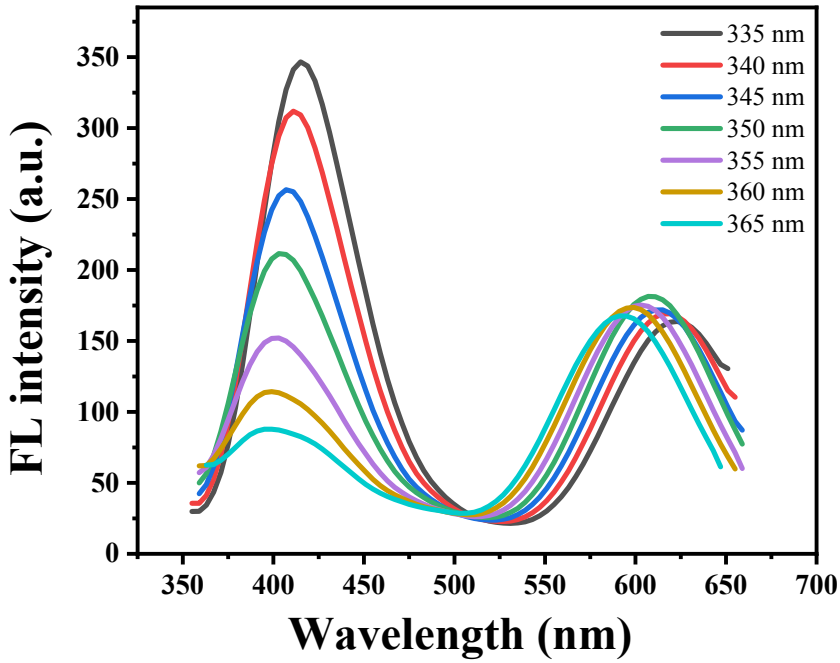

Fig. S4. Fluorescence emission spectra of CDs-Cu NCs in mixing ratio of 2:3 under different excitations (pH 6.80).

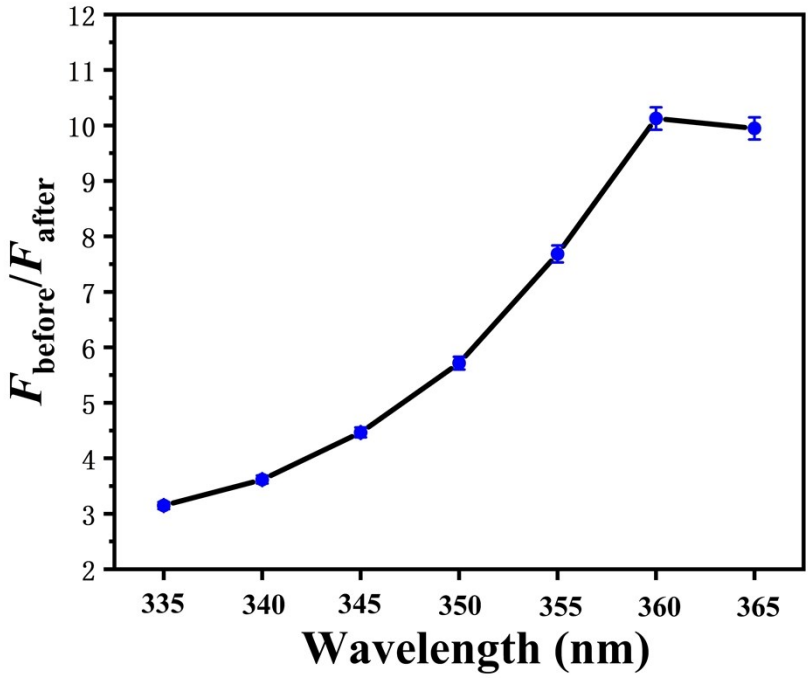

Fig. S5. The quenching efficiency of CDs–Cu NCs to Fe^{3+} with different excitation wavelengths (335–365 nm). In which F_{before} represent the ratio fluorescence intensities of CDs–Cu NCs (F_{624}/F_{424}) before addition of Fe^{3+}; F_{after} represent the ratio fluorescence intensities of CDs–Cu NCs (F_{624}/F_{424}) after addition of Fe^{3+} (40 μM).

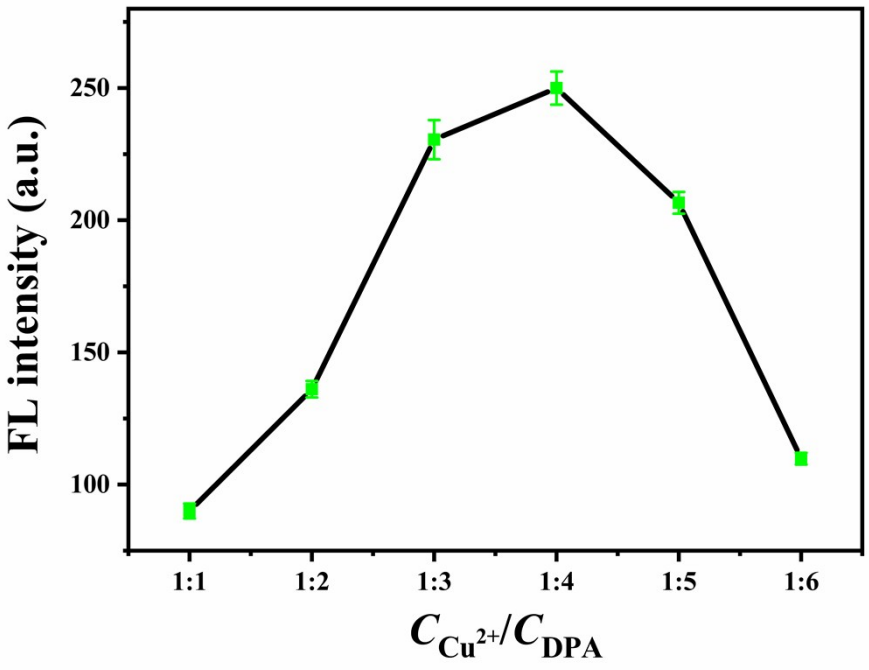

Fig. S6. The relationship between Cu NCs fluorescence intensity and concentration ratio of DPA.

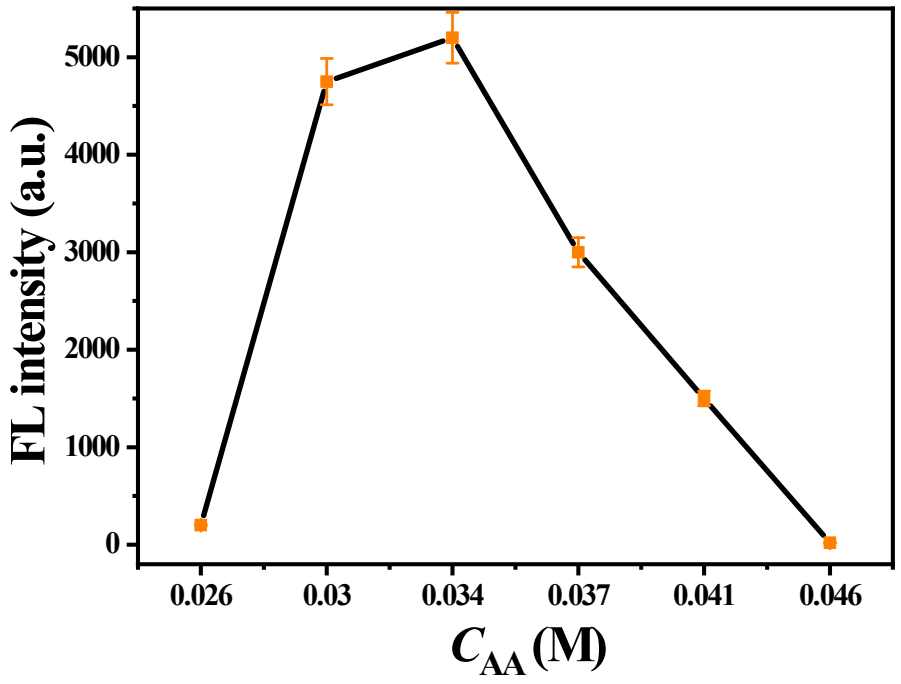

Fig. S7. The relationship between CDs fluorescence intensity and concentration ratio of AA.

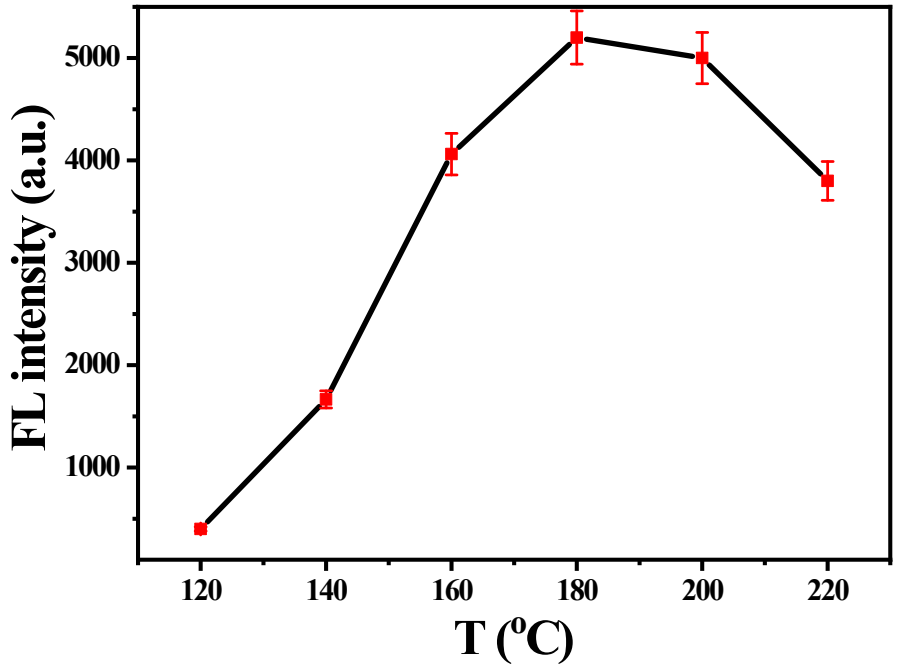

Fig. S8. Effect of synthesizing temperature of CDs on the fluorescence intensity.

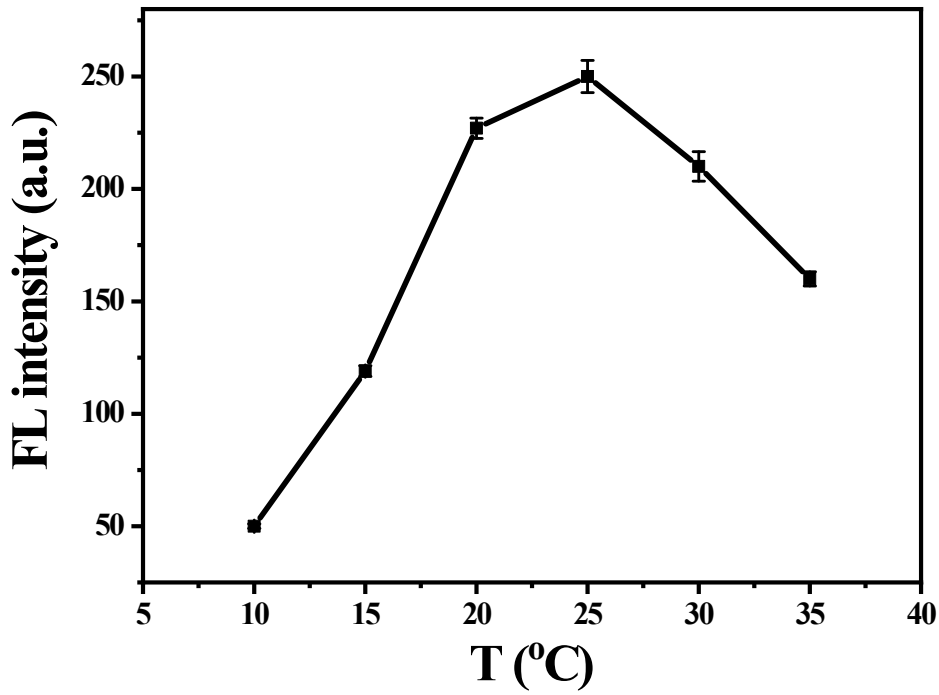

Fig. S9. Effect of synthesizing temperature of Cu NCs on the fluorescence intensity.

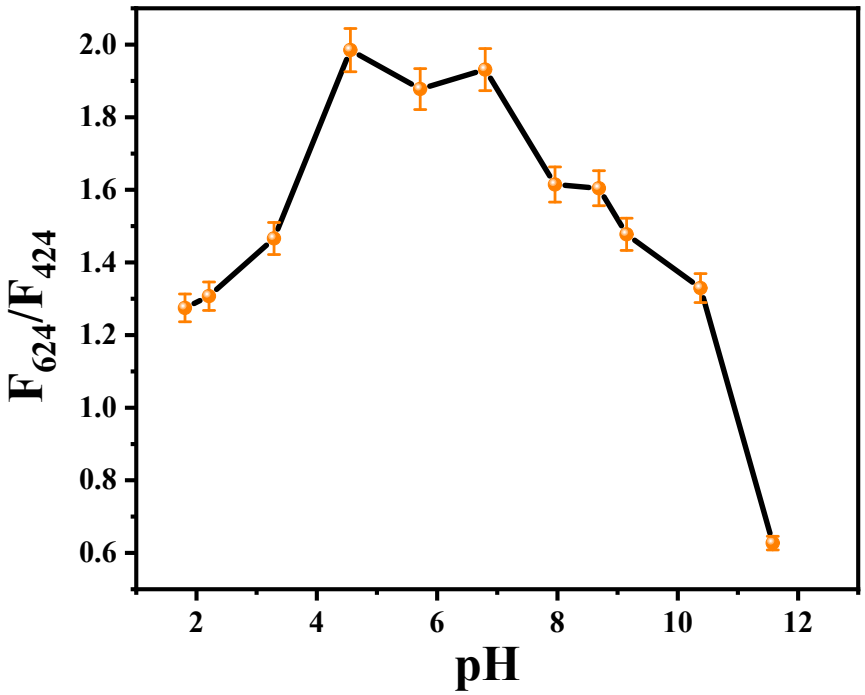

Fig. S10. Fluorescence quenching efficiency F_{624}/F_{424} of CDs–Cu NCs by Fe^{3+} (40 μM) at different pH values in the BR buffers (10 mM).

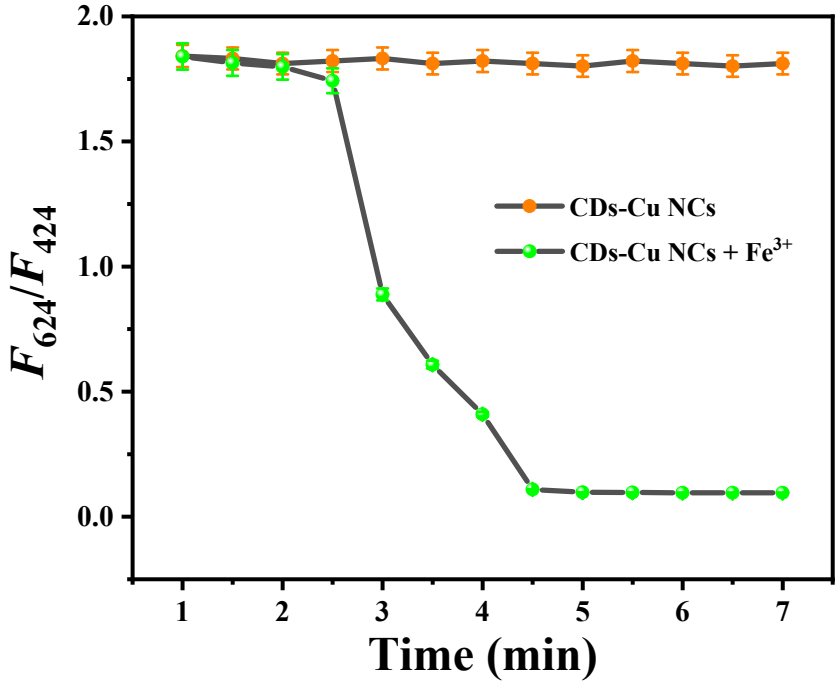

Fig. S11. Effect of reaction time on the fluorescence intensity of the CDs–Cu NCs/Fe^{3+} system at pH 6.80 (BR buffer, 10 mM).

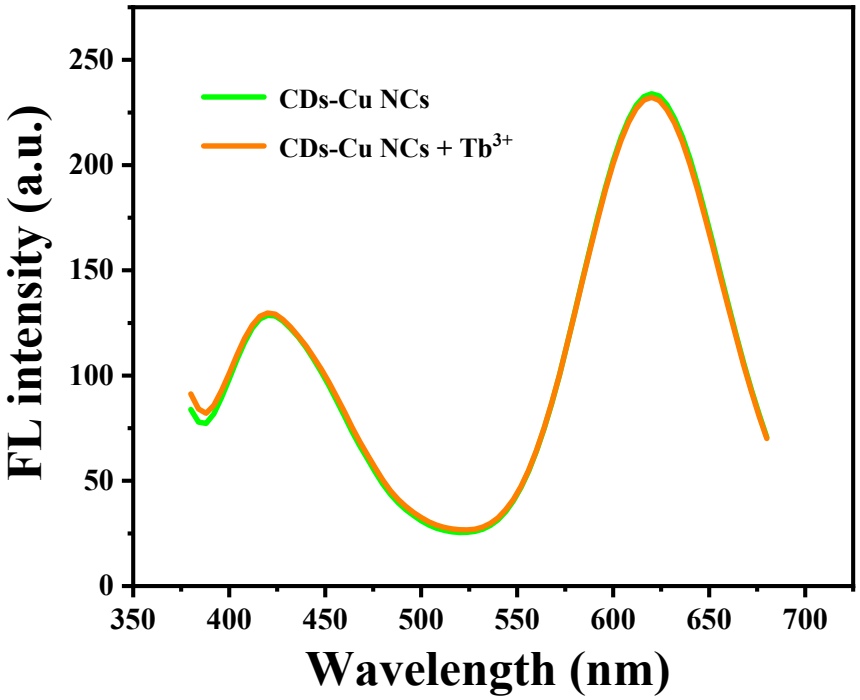

Fig. S12. The fluorescence intensity of the CDs–Cu NCs before and after the addition of Tb^{3+} at pH 6.80 (BR buffer, 10 mM).

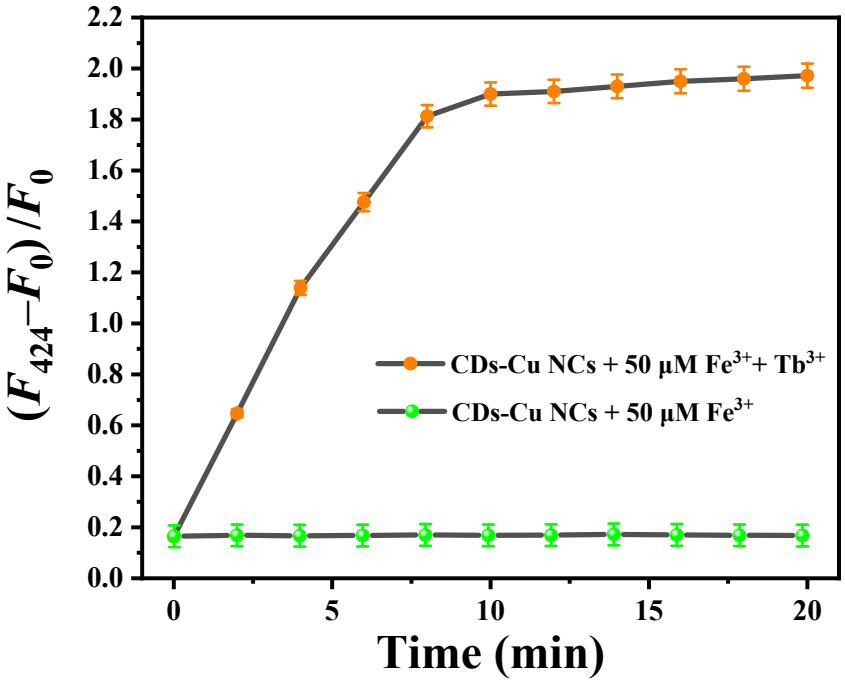

Fig. S13. Effect of reaction time on the fluorescence intensity of the CDs–Cu NCs/Fe^{3+} + Tb^{3+} system at pH 6.80 (BR buffer, 10 mM).

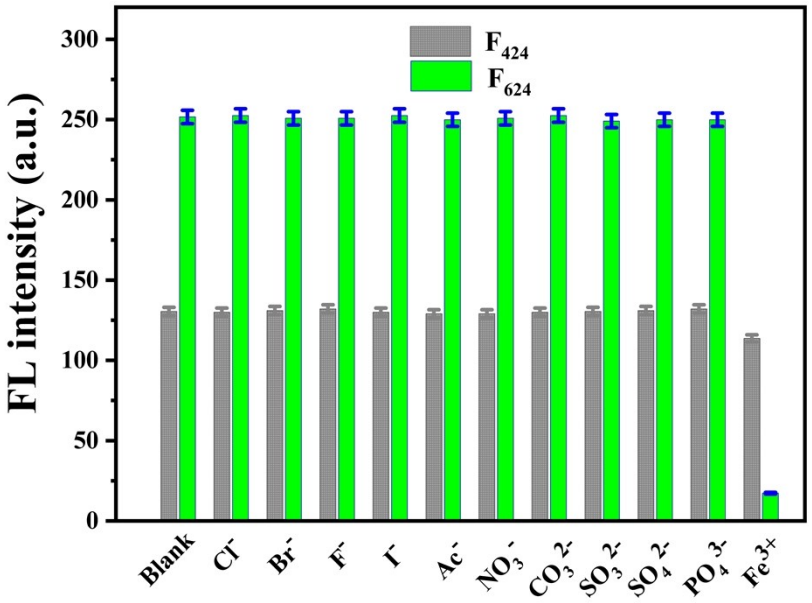

Fig. S14. Fluorescence responses of the CDs–Cu NCs (mixing ratio of 2:3) probe towards various anions (50 μM). (Conditions: BR buffer, pH 6.80; excitation, 360 nm.)

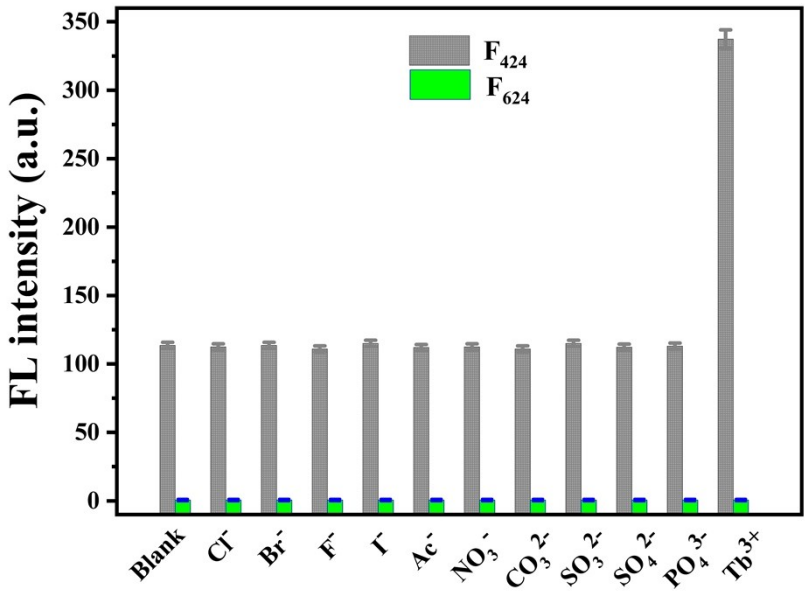

Fig. S15. Fluorescence responses of the CDs–Cu NCs/Fe^{3+} system towards various anions (50 μM). (Conditions: BR buffer, pH 6.80; excitation, 360 nm.)

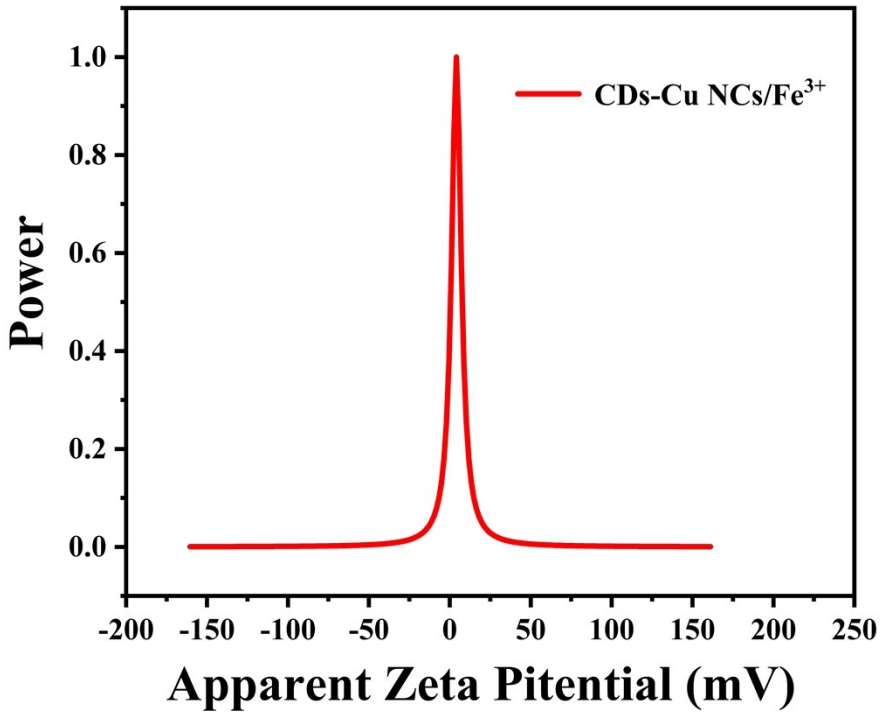

Fig. S16. Zeta potential of CDs-Cu NCs in the presence of Fe^{3+} ions (40 μM).

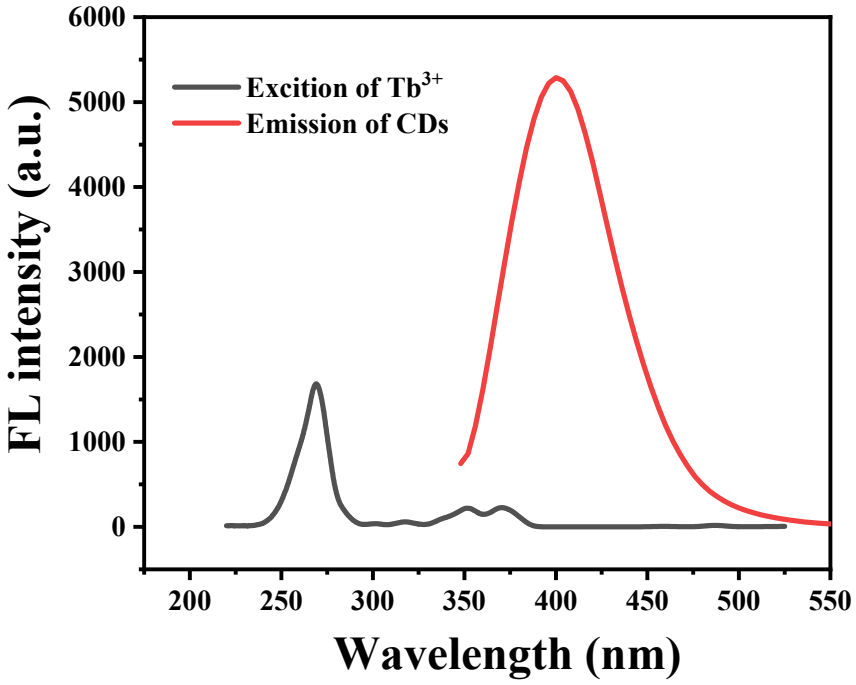

Fig. S17. Excitation spectrum of Tb^{3+} at the emission wavelength of 540 nm, and emission spectrum of CDs at the excitation wavelength of 360 nm.

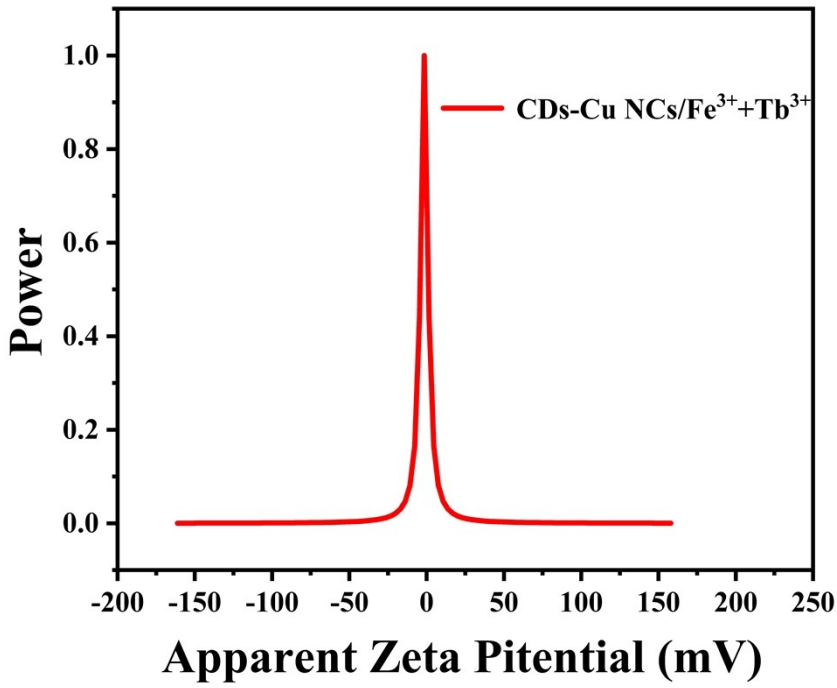

Fig. S18. Zeta potential of CDs-Cu NCs/Fe^{3+} in the presence of Tb^{3+} ions (50 μM).

Table S1 Results of the determination of Fe^{3+} in tap water and Yellow River water samples (n = 3).

Sample	Added (μM)	Found (μM)	Recovery (%)	RSD (%)
Tap water	0	ND [a]	/	/
	0.5	0.52	104.0	4.18
	10	10.34	103.4	3.02
	20	19.85	99.25	2.19
Yellow River water	0	2.60	/	/
	0.5	3.08	96.0	3.51
	10	12.33	97.3	2.76
	20	22.96	101.8	3.35

[a] not detected.